Autosomal dominant Zellweger spectrum disorder caused by de novo variants in PEX14 gene

H. R. Waterham, J. Koster, M. S. Ebberink, P. Ješina, J. Zeman, L. Nosková, S. Kmoch, P. Devic, D. Cheillan, R. J. A. Wanders, et al.

Genetics in Medicine (2023) 25, 100944

ELSEVIER

Genetics in Medicine
An Official Journal of the ACMG

www.journals.elsevier.com/genetics-in-medicine

ARTICLE

Autosomal dominant Zellweger spectrum disorder caused by de novo variants in *PEX14* gene

Hans R. Waterham[1,2,3,4,*], Janet Koster[1], Merel S. Ebberink[1], Pavel Ješina[5], Jiri Zeman[5], Lenka Nosková[5], Stanislav Kmoch[5], Perrine Devic[6], David Cheillan[7], Ronald J.A. Wanders[1,2,3,4], Sacha Ferdinandusse[1,2]

ARTICLE INFO

Article history:
Received 19 August 2022
Received in revised form
19 July 2023
Accepted 19 July 2023
Available online 23 July 2023

Keywords:
Peroxisome
Peroxisome biogenesis
Autophagy
Peroxisomal disorder
Metabolic disorder

ABSTRACT

Purpose: Zellweger spectrum disorders (ZSDs) are known as autosomal recessive disorders caused by defective peroxisome biogenesis due to bi-allelic pathogenic variants in any of at least 13 different *PEX* genes. Here, we report 2 unrelated patients who present with an autosomal dominant ZSD.

Methods: We performed biochemical and genetic studies in blood and skin fibroblasts of the patients and demonstrated the pathogenicity of the identified *PEX14* variants by functional cell studies.

Results: We identified 2 different single heterozygous de novo variants in the *PEX14* genes of 2 patients diagnosed with ZSD. Both variants cause messenger RNA mis-splicing, leading to stable expression of similar C-terminally truncated PEX14 proteins. Functional studies indicated that the truncated PEX14 proteins lost their function in peroxisomal matrix protein import and cause increased degradation of peroxisomes, ie, pexophagy, thus exerting a dominant-negative effect on peroxisome functioning. Inhibition of pexophagy by different autophagy inhibitors or genetic knockdown of the peroxisomal autophagy receptor NBR1 resulted in restoration of peroxisomal functions in the patients' fibroblasts.

Conclusion: Our finding of an autosomal dominant ZSD expands the genetic repertoire of ZSDs. Our study underscores that single heterozygous variants should not be ignored as possible genetic cause of diseases with an established autosomal recessive mode of inheritance.

Introduction

Peroxisomes play an essential role in a variety of metabolic pathways, including β-oxidation of very long-chain fatty acids (VLCFAs) and branched-chain fatty acids, α-oxidation of phytanic acid, and synthesis of ether-(phospho)lipids and primary bile acids.[1] Their number, protein content, and functions are controlled by de novo protein synthesis and organelle division and turnover.[2-5]

Defects in genes encoding peroxisomal proteins can cause different peroxisomal disorders, including single peroxisomal enzyme deficiencies, with only 1 specific

The Article Publishing Charge (APC) for this article was paid by Hans R. Waterham.

*Correspondence and requests for materials should be addressed to Hans R. Waterham, Laboratory Genetic Metabolic Diseases (F0-222), Amsterdam UMC – AMC, Meibergdreef 9, 1105 AZ Amsterdam, The Netherlands. *Email address:* h.r.waterham@amsterdamumc.nl

Affiliations are at the end of the document.

doi: https://doi.org/10.1016/j.gim.2023.100944

metabolic pathway affected, and peroxisome biogenesis disorders, characterized by a generalized defect in function, assembly, and propagation of peroxisomes.[6-8] The peroxisome biogenesis disorders comprise disorders with defective peroxisomal protein import, as in the Zellweger spectrum disorders (ZSDs) and Rhizomelic chondrodysplasia punctata type 1 and 5, and disorders with defective peroxisome division.[6,8]

The clinical severity of ZSDs ranges from an early lethal presentation to a late-onset, often progressive neurological disease or even isolated hearing and/or vision deficits.[7] Because of the generalized peroxisomal protein import defect in ZSD cells, all peroxisome-dependent metabolic pathways do not function properly, resulting in characteristic metabolic aberrations, which, combined, are diagnostic for ZSDs. These include accumulation of VLCFAs, branched-chain fatty acids and bile-acid precursors, and a deficiency of ether (phospho)lipids.[6,9] All ZSDs reported so far are autosomal recessive disorders caused by bi-allelic pathogenic variants in any of at least 13 different *PEX* genes.[6,10] The encoded PEX proteins are involved in the targeting and/or import of matrix proteins into the peroxisomal lumen, or in the targeting and/or insertion of membrane proteins into the peroxisomal membrane. Targeting and import of matrix proteins involves recognition of newly synthesized proteins by the cytosolic receptor proteins PEX5 or PEX7, docking of the cargo-loaded receptor proteins onto the PEX13-PEX14 docking complex in the peroxisomal membrane, import of the matrix proteins and ubiquitination of PEX5 by the PEX2-PEX10-PEX12 complex in the peroxisomal membrane, and finally, release and recycling of the receptor proteins by the PEX1-PEX6-PEX26 complex, which is tethered via PEX26 to the peroxisomal membrane.[5,6] Severe bi-allelic pathogenic variants in any of these 10 *PEX* genes abrogates peroxisomal matrix protein import and results in peroxisomal membrane vesicles that still contain membrane but no matrix proteins and which are also referred to as peroxisomal ghosts.[10] Targeting and insertion of peroxisomal membrane proteins involves PEX19 as cytosolic receptor protein, PEX3 as docking protein for cargo-loaded PEX19, and PEX16 as possible receptor for PEX3.[5,6] Severe bi-allelic pathogenic variants in *PEX3*, *PEX16*, or *PEX19* abrogates both peroxisomal matrix and membrane protein import, resulting in a complete absence of peroxisomal membrane vesicles.[10]

Here, we report 2 unrelated male patients with progressive neurological symptoms that are compatible with a peroxisomal disorder. Laboratory diagnosis suggested the diagnosis ZSD. Genetic testing identified different single heterozygous de novo variants in *PEX14* of each of the 2 patients, which both result in the synthesis of similar C-terminally truncated PEX14 proteins. Detailed functional studies showed that the truncated PEX14 proteins have a dominant-negative effect on peroxisome functioning.

Materials and Methods

Cell culturing

Primary skin fibroblasts derived from the 2 patients (patient 1 and patient 2), 2 PEX14-null patients (PEX14(1)[11] and PEX14(2)[12]), 1 PEX13-null patient (PEX13[13]), and 2 healthy individuals (Control 1 and Control 2), and HeLa cells and HEK 293 cells were cultured in Dulbecco's modified Eagle's medium (Gibco) plus 25 mM of HEPES buffer (VWR) containing 10% fetal bovine serum, 100 U/mL penicillin, and 100 µg/mL streptomycin (Gibco), in a humidified atmosphere of 5% CO2 at 37 °C or for 7 days at 40 °C.

Biochemical analysis

Cellular levels of VLCFAs C22:0, C26:0,[14] and C26:0-lysophosphatidylcholine (C26:0-lysoPC)[15] and the activity of dihydroxyacetone phosphate acyltransferase (GNPAT)[16] were measured as previously described. Cellular peroxisomal β-oxidation and fatty acid elongation capacities were determined using the D_3-C22:0 loading test.[17] Peroxisome-dependent de novo ether-(phospho)lipid synthesis was assessed by measuring the levels of the ether-phospholipids PC-(O-37:4) and PE-(O-39:7) after incubation of cells with 40 µM 1-heptadecanol (C17:0-OH) for 24 hours.[18]

Immunofluorescence microscopy

Immunofluorescence microscopical analysis of peroxisomes was performed[19] using antibodies raised against catalase (mouse monoclonal, own production, Mab 17E10; diluted 1:3),[20] ABCD3 (rabbit polyclonal, Thermo Fisher PA1-650; diluted 1:500), ACBD5 (rabbit polyclonal, Sigma HPA012145; diluted 1:500), or PEX5 (rabbit polyclonal; gift of G. Dodt; diluted 1:800). Biotinylated goat anti-mouse (DAKO; diluted 1:200) plus streptavidin-FITC (ThermoFisher; diluted 1:200), and Alexa Fluor goat anti-rabbit 594 (Invitrogen; diluted 1:500) were used as secondary antibodies. Cells were analyzed with a Zeiss Axio Observer A1 fluorescence microscope.

Genetic analysis

For patient 1, the coding and flanking intron sequences of the 13 currently known *PEX* genes were Sanger sequenced following polymerase chain reaction amplification of genomic DNA isolated from primary skin fibroblasts.[13] Patient 1 was also subjected to exome sequencing as previously described using SeqCap EZ MedExome Probes (Roche) and a Novaseq 6000 platform (Illumina).[21]

For patient 2, genomic DNA isolated from primary skin fibroblasts was analyzed by in-house peroxisomal gene panel sequencing (IonTorrent; ThermoFisher), including all 13 currently known *PEX* genes.

Total complementary DNA (cDNA) was prepared from RNA isolated from primary skin fibroblasts by trizol extraction (Sigma-Aldrich) using the QuantiTect Reverse Transcription Kit (QIAGEN). *PEX14* cDNA (GenBank accession number NM_004565.2) was polymerase chain reaction amplified using *PEX14*-specific primer pairs followed by Sanger sequencing.[13]

Complementation testing of primary skin fibroblasts by means of *PEX* cDNA transfection has been described previously.[13]

Immunoblotting

Cells were lysed in a phosphate-buffered saline solution containing 0.1% sodium dodecyl sulfate and Complete Mini protease inhibitors (Roche). Proteins were separated by nuPAGE (Invitrogen) and transferred onto nitrocellulose. Immunoblot analysis was performed with rabbit polyclonal antibodies against PEX14 (gift from M. Fransen; diluted 1:1,000), peroxisomal 3-ketoacyl-CoA thiolase (Atlas antibodies HPA007244; diluted 1:2,000), ACOXI (Abcam ab184032; diluted 1:2,000), ABCD1 (Euromedex; diluted 1:500), ABCD3 (Thermo Fisher PA1-650; diluted 1:2,000), ACBD5 (Sigma-Aldrich HPA012145; diluted 1:500), PEX5 (Sigma HPA039259; diluted 1:500), PEX13 (gift from D. Crane; diluted 1:1,000), PEX19 (Sigma-Aldrich; diluted 1:1,000), LC3B (Abcam ab48394; diluted 1:1,500), or SQSTM1/P62 (BD Transduction lab; diluted 1:2,000). For control of equal loading, monoclonal antibodies against β-actin (Sigma-Aldrich; diluted 1:10,000) or α-tubulin (Sigma-Aldrich; diluted 1:2,000) were used. Detection was done after incubation with secondary antibodies IRDye 800CW goat anti-rabbit, IRDye 800CW goat anti-mouse, or IRDye 680RD donkey anti-mouse (all diluted 1:10,000) on the Odyssey Infrared Imaging System (LI-COR Biosciences).

PEX14 overexpression

The truncated PEX14 protein of patient 1 was stably expressed in HeLa cells under transcriptional control of the cytomegalovirus promoter following genomic insertion of the encoding DNA sequence into a FlpIn site. To this end, *PEX14* with the 37 base pair insertion was amplified from total cDNA prepared from RNA isolated from patient 1's fibroblasts, sub-cloned into the pcDNA5/FRT vector (Invitrogen) and verified by Sanger sequencing. The construct was transfected into HeLa-FlpIn cells, which were selected for 1 month on 150 μg/mL hygromycin (Sigma-Aldrich).

PEX14 pull-down experiments

The coding sequences for wild-type PEX14 (PEX14-wt) and truncated PEX14 of patient 1 (PEX14-trunc) were sub-cloned into the pCMV-Tag2b vector (Agilent Technologies) creating 5' FLAG-tagged versions. The constructs and, as control, the pCMV-Tag2b vector without insert were co-transfected separately with PEX19-pcDNA3 into HEK 293 cells using Lipofectamine 2000 (Invitrogen). Forty-eight hours after transfection, immunoprecipitation was performed using anti-FLAG M2 agarose beads (Sigma-Aldrich). The immunoprecipitates were analyzed by immunoblotting as described above.

Pexophagy assay

To assess pexophagy in the fibroblasts, we used the previously described Red-Green lysosome pexophagy assay.[22] In brief, fibroblasts were transiently transfected with a plasmid encoding the peroxisomal reporter mCherry–GFP-SKL using the AMAXA NHDF Nucleofector Kit (Lonza) according to the manufacturer's instructions. Following transfection, cells were cultured at 37 °C in live cell chambers (μ-Slide 4 Well Glass Bottom, Ibidi GmbH), and 24 hours after transfection incubated for 4 days with lysosomal protease inhibitors in order to prevent mCherry–GFP degradation in the lysosome (2 μM E-64 and 500 μM leupeptin (Enzo Life Sciences). Cells were then imaged with a Leica TCS SP8 filter-free spectral confocal microscope and images were processed as described in detail in.[22] Three independent experiments were performed and 25-40 images of cells per condition were acquired in different areas of the live cell chambers. For each fibroblast cell line, we analyzed 100 cells in total; pexophagy-induced fibroblasts were defined as having >20% "red-only" pixels.[22]

Autophagy inhibition

To inhibit autophagy, including pexophagy, we incubated fibroblasts for 7 days with 10 mM 3-methyladenine (3-MA; Sigma M9281) or 10 μM chloroquine (CQ; Sigma C6628) as previously described.[18,23] In addition, we generated fibroblasts that stably express short hairpin RNAs against *NBR1* as previously described.[18] Finally, we incubated fibroblasts for 4 days in the presence of 2 μM E-64 and 500 μM leupeptin, similar as described above for the Red-Green lysosome pexophagy assay. Cells were examined by immunofluorescence microscopy, immunoblot, and/or biochemical analyses as described above.

Statistics

Statistical significance of data was evaluated using GraphPad Prism. Statistical tests of choice are indicated in the figure legends.

Results

Biochemical and genetic analysis of patients' cells

Clinical features in combination with mildly aberrant peroxisomal metabolite levels in plasma suggested a mild

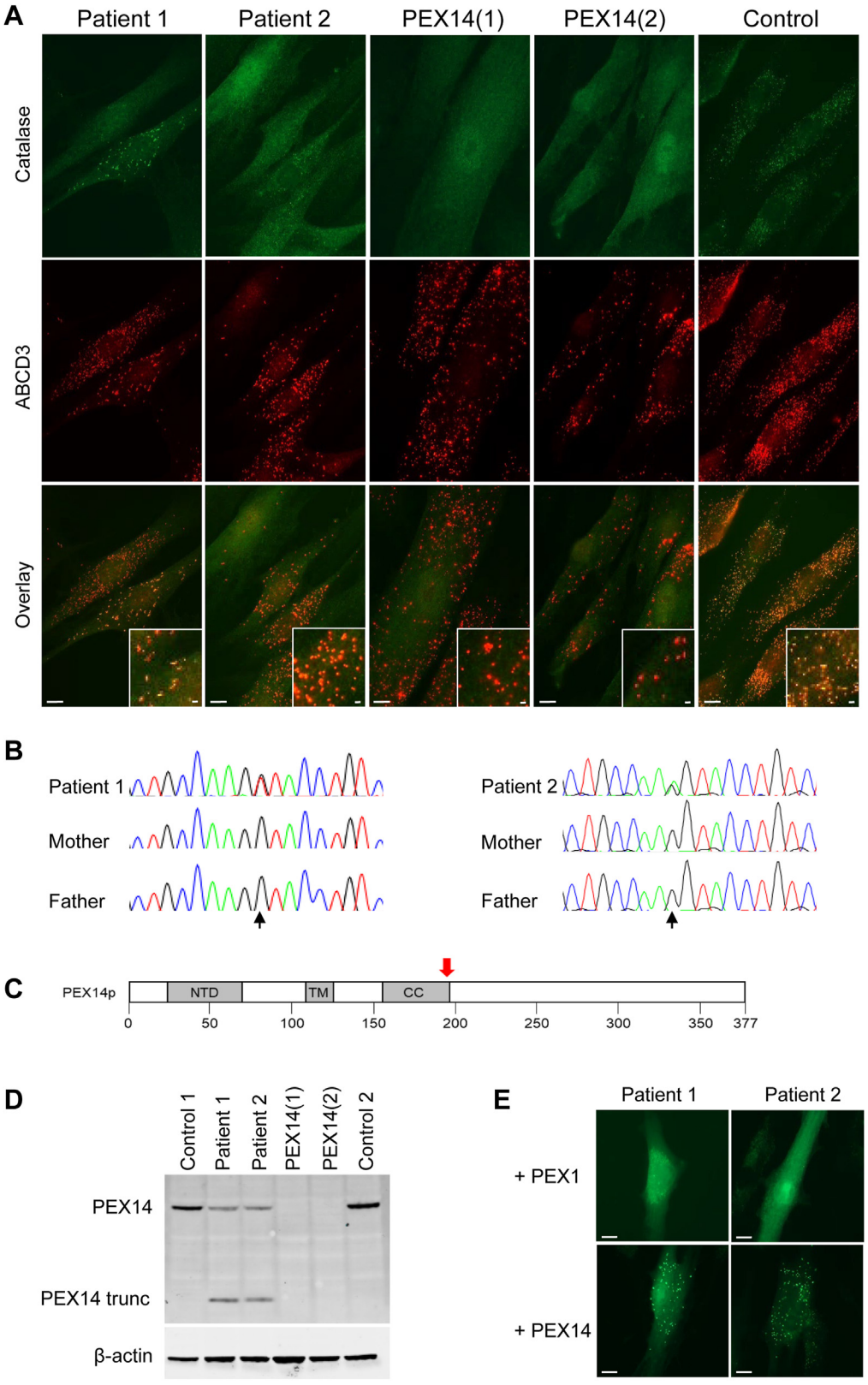

Figure 1 Analysis of patients' fibroblasts. A. Immunofluorescence microscopy analysis to determine the subcellular location of the peroxisomal matrix protein catalase (green signal) and the peroxisomal membrane protein ABCD3 (red signal) in primary fibroblasts of the 2 heterozygous PEX14 patients (patient 1 and 2), 2 previously reported PEX14-null patients (PEX14(1) and PEX14(2)), and a control individual. Shown are representative images (scale bar, 10 μm). B. Electropherograms showing the Sanger sequencing results of patient 1 and patient 2 and their respective parents. Both patients are heterozygous for a de novo *PEX14* variant (location indicated by arrows). Patient 1 is heterozygous for NC_000001.11(NM_004565.2):c.585+1G>T and patient 2 is heterozygous for NM_004565.2:c.585G>A. C. Schematic

peroxisomal disorder in 2 male patients, who currently are both in their twenties (summarized in Supplemental information and Table 1A). Biochemical analyses in primary skin fibroblasts of both patients subsequently showed an abnormal VLCFA profile with increased C26:0 and C26:0-lysoPC levels, an abnormal D_3C22:0 loading test with decreased peroxisomal β-oxidation capacity and increased chain-elongation to D_3C26:0, a low activity of the peroxisomal enzyme GNPAT (involved in ether-(phospho) lipid synthesis), and a marginally lowered de novo ether-(phospho)lipid synthesis (reflected by reduced PC-(O-37:4) and PE-(O-39:7) levels) (Supplemental Table 1B). Combined, these findings indicated that both patients suffered from a mild ZSD.

Immunofluorescence microscopy of the patients' fibroblasts using antibodies against the peroxisomal matrix protein catalase and the peroxisomal membrane protein ABCD3 revealed a majority of cells with catalase localized in peroxisomes, as judged from its co-localization with ABCD3, as well as in the cytosol, and ~20% of cells with catalase completely mislocalized to the cytosol, and the number of ABCD3-stained peroxisomal vesicles per cell reduced (Figure 1A; see also Figures 4B and 5B for quantifications). This heterogeneous cellular phenotype resembles the previously described peroxisomal catalase-import mosaicism, which is often observed in cells of ZSD patients with an attenuated phenotype.[13,24,25] For comparison, we included 2 PEX14-null fibroblasts in which catalase was cytosolic in all cells, in agreement with PEX14's role in peroxisomal matrix protein import. A subset of PEX14-null cells showed a reduced number of ABCD3-stained peroxisomal vesicles, albeit less reduced as observed in the catalase-import-deficient patients' cells.

The peroxisomal mosaic phenotype complicated identification of the defected *PEX* gene by means of complementation testing of the cells using *PEX* cDNA transfection.[13] We therefore Sanger sequenced all 13 known *PEX* genes in patient 1 and performed panel sequencing of 26 genes encoding peroxisomal proteins, including all *PEX* genes, in patient 2. We found both patients heterozygous for a single variant in *PEX14*: patient 1 for an NC_000001.11(NM_004565.2):c.585+1G>T and patient 2 for an NM_004565.2:c.585G>A variant (Figure 1B). Additional exome sequencing of patient 1 confirmed the heterozygous *PEX14*-c.585+1G>T variant and did not identify additional pathogenic variants in any of the *PEX* genes, including *PEX14*. Both *PEX14* variants are located in the splice donor site of intron 7 and predicted to affect *PEX14* messenger RNA (mRNA) splicing. They are not listed in the gnomAD, ExAC, or ClinVar databases.

The finding of only 1 single heterozygous *PEX14* variant in each of the 2 patients does not correspond with an autosomal recessive mode of inheritance, which is common for ZSDs. Moreover, the variants were absent in the parental DNAs, indicating that they arose de novo in the patients (Figure 1B). *PEX14* cDNA analysis of reverse transcribed RNA isolated from the patients' cells revealed normal expression of the wild-type *PEX14* alleles and confirmed that both variants cause aberrant splicing, each resulting in a stable *PEX14* mRNA with the same retention of 37 base pairs of intron 7 sequence: r.585_586insuuaccugucucugcugcacagggcccuccaggcccag for patient 1 and r.585delinsaguaccugucucugcugcacagggcccuccaggcccag for patient 2. This retention causes a shift of reading frame predicted to result in 2 nearly identical, severely truncated PEX14 proteins of 230 amino acids, which have the alanine at amino acid position 196 substituted for a leucine or a valine, and the C-terminal 181 amino acids of wild-type PEX14 substituted for the same 34 amino acids: p.A196Lfs*34 for patient 1 and p.A196Vfs*34 for patient 2 (Figure 1C). Although such truncated proteins are often degraded, the truncated PEX14 proteins appear as stable as the wild-type PEX14 proteins produced from the *trans PEX14* allele in the patients' cells (Figure 1D).

To confirm that the aberrant peroxisomal phenotype in the patients' cells is indeed due to a defective *PEX14*, we cultured the patients' cells at 40 °C to aggravate the peroxisomal phenotype (explained below) and then co-transfected the cells with the peroxisomal reporter protein GFP-PTS1 and wild-type *PEX14* or, as a control, wild-type *PEX1* cDNA.[13] Three days after transfection, we observed GFP-PTS1-containing peroxisomes in approximately 20% of the cells co-transfected with *PEX14* cDNA, whereas co-transfection with *PEX1* cDNA did not result in GFP-PTS1-containing peroxisomes (Figure 1E).

Taking these results together, we considered the heterozygous *PEX14* variants as likely pathogenic and hypothesized that the truncated PEX14 proteins have a dominant-negative effect on peroxisome function and appearance.

presentation of PEX14 protein indicating the locations of the N-terminal domain (NTD), previously shown to interact with PEX5, PEX13, and PEX19, the trans-membrane domain (TM), the coiled coil domain (CC), shown to be involved in PEX14 dimerization, and the location of the *PEX14* variants found in the patients causing the truncation of the encoded PEX14 protein (red arrow): p.A196Lfs*34 for patient 1 and p.A196Vfs*34 for patient 2. D. Immunoblot analysis of homogenates prepared from primary fibroblasts of the 2 heterozygous PEX14 patients, 2 previously reported PEX14-null patients, and 2 control individuals. The upper panel shows the immunoblot using antibodies against PEX14 and the lower panel the same blot re-probed with antibodies against β-actin as loading control. Performed in triplicate; shown are representative immunoblots. E. Fluorescence microscopy analysis to determine the subcellular location of GFP-PTS1 in primary fibroblasts of the 2 heterozygous PEX14 patients cultured at 40 °C and co-transfected with cDNAs encoding PEX1 and GFP-PTS1 or PEX14 and GFP-PTS1. Shown are representative images 3 days after transfection (scale bar, 10 μm).

Truncated PEX14 proteins have a dominant-negative effect on peroxisome function and appearance

To further confirm the pathogenic nature of the truncated PEX14 proteins we expressed truncated PEX14 of patient 1 (PEX14-trunc) in PEX14-null fibroblasts, which, in contrast to wild-type PEX14, did not result in restoration of the defective peroxisomal matrix protein import in these cells (not shown). Next, we stably expressed PEX14-trunc or, as a control, wild-type PEX14 (PEX14-wt) in wild-type HeLa cells (which also express endogenous PEX14). The expression of PEX14-trunc, but not of PEX14-wt, resulted in a peroxisomal mosaic phenotype similar as observed in the patients' fibroblasts (Figure 2A), which thus confirmed that PEX14-trunc has a dominant-negative effect on the function and appearance of peroxisomes.

The amino-terminal half of PEX14 was previously shown to physically interact with PEX5, PEX19, PEX13, and itself (Figure 1C, and reviewed in [26]). To study whether the truncated PEX14 proteins can still interact with these partner proteins, we performed pull-down experiments with HEK 293 cells expressing FLAG-tagged PEX14-trunc or PEX14-wt. After pull-down of the FLAG-tagged PEX14 proteins using FLAG-specific antibodies followed by immunoblot analysis, we did not observe a difference between PEX14-trunc and PEX14-wt with respect to binding of PEX5, PEX9, PEX13, and PEX14 (Figure 2B).

Finally, we looked for the subcellular location of PEX5 protein in the patients' cells. Previous reports have shown that PEX5 is predominantly cytosolic in control cells but accumulates at the membrane of peroxisomal ghosts in patients' cells defective for certain *PEX* genes, including *PEX2* and *PEX12*[27] and *PEX1*, *PEX6*, and *PEX26*.[23] Surprisingly and opposite to what has been reported previously in mutant Chinese hamster ovary (CHO) cells,[28] we found that PEX5 accumulates at the peroxisomal membrane in all PEX14-null cells but is cytosolic in PEX13-null cells. In contrast to the PEX14-null cells, we found PEX5 to be mainly cytosolic in the cells of both patients similar to the control cells (Figure 2C). This indicates that cycling of the PEX5 receptor still occurs efficiently in the patients' cells.

Taken together, these findings show that PEX14-trunc is stably expressed, can still bind with its known partner proteins, and does not appear to prevent cycling of the PEX5 receptor in the patients' cells. However, PEX14-trunc alone cannot functionally rescue PEX14-null cells and, when co-expressed with wild-type PEX14, results in a peroxisomal mosaic phenotype.

Truncated PEX14 proteins cause increased peroxisome degradation

The peroxisomal mosaic phenotype in cells expressing both truncated and wild-type PEX14 resembles the peroxisomal catalase-import mosaicism observed in cells from ZSD patients with an attenuated phenotype.[24,25] When such cells are cultured at an elevated temperature, they usually show a more severe peroxisomal phenotype, including, in particular, the (near) complete loss of peroxisomal catalase import.[10] Culturing the fibroblasts of the heterozygous PEX14 patients at 40 °C for 7 days also caused a nearly complete disappearance of the peroxisomal mosaic phenotype with catalase present in the cytosol of most cells (Figure 3A). In addition, however, a further reduction in overall ABCD3 staining and an increased number of cells completely lacking ABCD3 staining was observed. This was remarkable, because PEX14 is known to play only a role in the import of peroxisomal matrix proteins but not of peroxisomal membrane proteins. Indeed, in PEX14-null cells, catalase is also cytosolic, but ABCD3 is still abundantly present in the peroxisomal vesicles of all cells (Figure 3A). These findings therefore suggested that the truncated PEX14 proteins cause either a block of both peroxisomal matrix and membrane protein import or increased degradation of peroxisomes, and this effect is enhanced at elevated temperatures.

To study this further, we first determined by immunoblot analysis the fate of PEX14 protein in the patients' cells cultured at 40 °C. We found a marked reduction in the levels of both wild-type and truncated PEX14 protein when compared with patients' cells cultured at 37 °C. This temperature-induced reduction was not observed in control cells (Figure 3B). Next, we studied the effect of elevated temperature on peroxisomal matrix protein import in the patients' cells using the processing of Acyl-CoA oxidase (ACOX1; PEX5-mediated import) and thiolase (PEX7-mediated import) as readout. As previously reported[18] and also shown in Figure 3C, both proteins are synthesized as larger precursor proteins that become processed only after import into the peroxisomal lumen, making their processing efficiency a sensitive readout for functional peroxisomal matrix import. We found that in both patients' cells the processing and thus peroxisomal import of both ACOX1 and thiolase was completely normal and similar as observed in the control cells. However, whereas the levels of processed thiolase in the patients' and the PEX14-null cells were already moderately decreased at 37 °C when compared with control cells, the levels of both processed thiolase and processed ACOX1 in the patients' cells, but not the PEX14-null cells, became markedly decreased when these cells were cultured at 40 °C (Figure 3C). Similarly, also for 2 known peroxisomal membrane proteins, ABCD1 and ACBD5, we noted moderately decreased levels at 37 °C and a marked decrease at 40 °C in the patients' cells when compared with control and PEX14-null cells (Figure 3D). This is in accordance with the decreased ABCD3 staining we observed in these cells (Figure 3A).

Taken together, these results strongly suggested that the defective peroxisomal functions in the patients' cells are not due to defective import of both peroxisomal matrix and membrane proteins but to an increased degradation of peroxisomes, which can be further enhanced at elevated temperature.

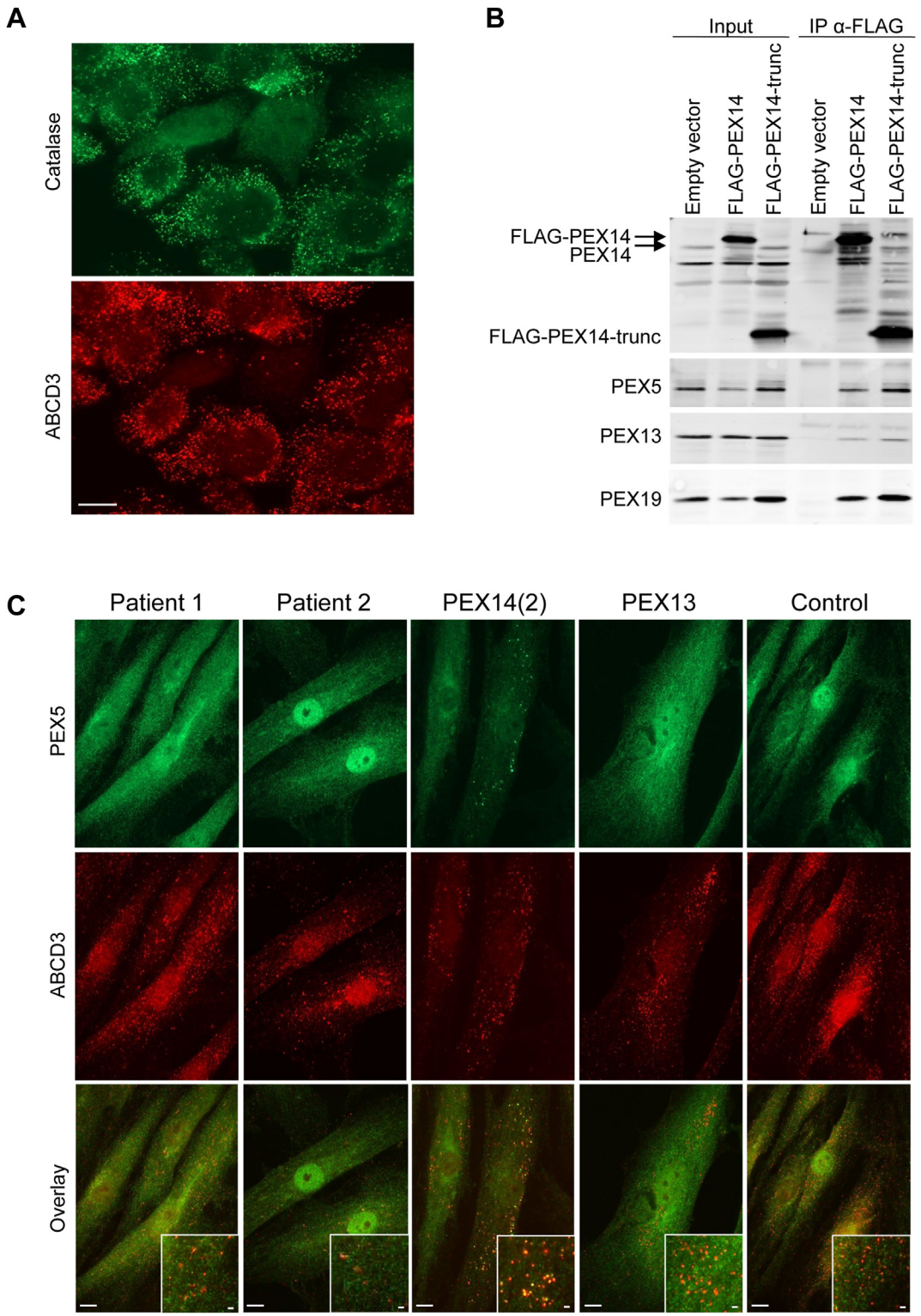

Figure 2 **Analysis of truncated PEX14 protein.** A. Immunofluorescence microscopy analysis of control HeLa cells transfected with a cDNA encoding PEX14-trunc results in a peroxisomal mosaic phenotype similar as observed in the patient cells (compare with Figure 1A) (scale bar, 10 µm). Transfection of HeLa cells with a cDNA encoding PEX14-wt does not result in a peroxisomal mosaic phenotype (not shown). B. Pull-down experiments with HEK 293 cells expressing FLAG-tagged PEX14-wt or FLAG-tagged PEX14-trunc. As a control, we included HEK 293 cells transfected with the expression vector lacking PEX14 (empty vector). FLAG-tagged PEX14 proteins and associated proteins were immunoprecipitated using FLAG-specific antibodies followed by immunoblot analysis of the immunoprecipitates using antibodies against PEX5, PEX13, PEX14, and PEX19. Performed in triplicate; shown are representative immunoblots. C. Immunofluorescence microscopy analysis to determine the subcellular location of the peroxisomal matrix protein import receptor PEX5 (green signal) in primary fibroblasts of the heterozygous PEX14 patients, a PEX14-null patient (PEX14(2)), a PEX13-null patient, and a control individual. Peroxisomal membranes are stained with antibodies against the peroxisomal membrane protein ABCD3 (red signal). Shown are representative images (scale bar, 10 µm).

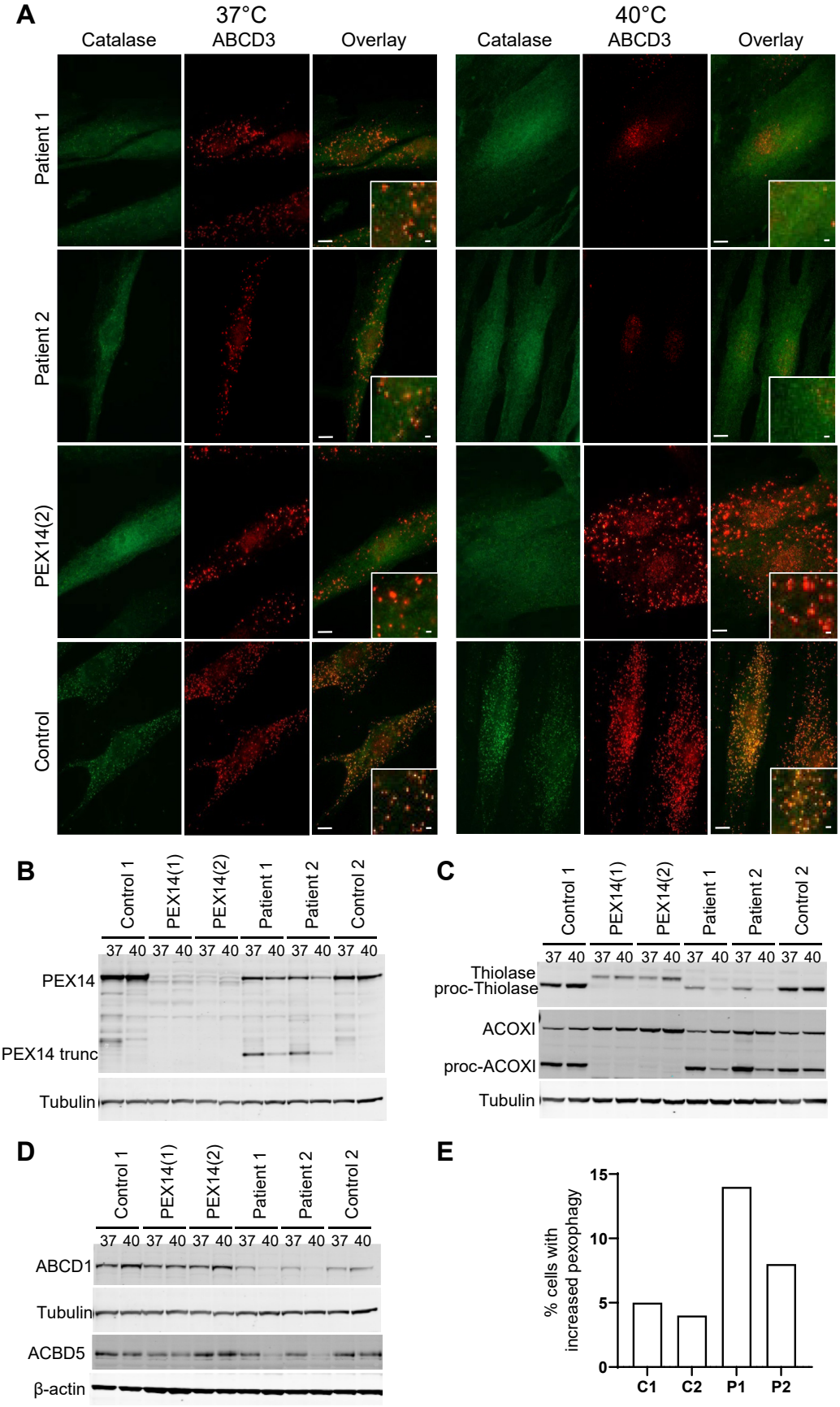
A
37°C
40°C
Catalase
ABCD3
Overlay
Patient 1
Patient 2
PEX14(2)
Control
B
Control 1
PEX14(1)
PEX14(2)
Patient 1
Patient 2
Control 2
37 40
PEX14
PEX14 trunc
Tubulin
C
Thiolase
proc-Thiolase
ACOXI
proc-ACOXI
Tubulin
D
ABCD1
Tubulin
ACBD5
β-actin
E
% cells with increased pexophagy
15
10
5
0
C1
C2
P1
P2

We hypothesized that this increased degradation occurs via increased selective autophagy, a cellular mechanism that normally removes unnecessary or nonfunctional organelles through inclusion in auto-phagosomes, which then fuse with lysosomes, after which the contents are degraded. This process has been well characterized and several key proteins and inhibitors of the process have been described.[3] Selective autophagy of peroxisomes is also known as pexophagy. In order to visualize and quantify the pexophagy activity in the patients' cells, we used the previously reported Red-Green lysosome pexophagy assay.[22,29] To this end, we cultured the 2 patient and 2 control cell lines, which transiently expressed the mCherry-GFP-SKL peroxisomal reporter, at 37 °C in the presence of lysosomal protease inhibitors to prevent the degradation of mCherry-GFP-SKL in the lysosome, followed by fluorescent microscopy. In this assay, peroxisomes that are not subject to pexophagy appear yellow/greenish labeled, whereas peroxisomes subject to pexophagy and fused with lysosomes appear as orange/red labeled because of quenching of the green (GFP) fluorescence in the acidic environment of the lysosome. We observed a clear increase in the number of patients' cells with increased pexophagy, ie, cells in which >20% of peroxisomes are orange/red labeled, when compared with the control cells (Figure 3E and Supplemental Figure 1).

Autophagy inhibition rescues peroxisomal functions in patients' cells

To find additional indications that the defective peroxisomal functions in the patients' cells are the consequence of increased pexophagy, we incubated the cells with the early autophagy inhibitor 3-methyladenine (3-MA) at 37 °C and 40 °C. To verify the inhibition by 3-MA, we assessed the levels of the autophagy adaptor protein SQSTM1/P62 (P62) and the levels and conversion of MAPILC3B-I (LC3I) to MAPILC3B-II (LC3II) by immunoblot analysis. Increasing the cell culturing temperature to 40 °C resulted in decreased P62 levels reflecting increased autophagy in all cell lines used (Figure 4A), whereas incubation of the cells with 3-MA resulted in increased P62 levels at 40 °C, as well as at 37 °C, confirming the inhibition of autophagy. In the presence of 3-MA, we no longer observed the reduction in the levels of processed thiolase and ABCD1 in the patient's cells, which we observed when the same cells were cultured in the absence of 3-MA (Figure 4A), strongly suggesting that autophagy is, indeed, involved. This effect was strongest in the cells cultured at 40 °C but also clearly visible in the cells cultured at 37 °C. Importantly, incubation of the patients' cells with 3-MA at 40 °C also resulted in a correction of the number of cells with catalase- and ABCD3-containing peroxisomes to the level observed in cells cultured at 37 °C without 3-MA (Figure 4B and Supplemental Figure 2). Finally, incubation of the patients' cells with 3-MA at 40 °C resulted in increased peroxisomal fatty acid β-oxidation capacities (D_3C16:0/D_3C22:0 ratio) and decreased levels of D_3C26:0, indicating that autophagy inhibition also restored peroxisomal metabolic functions (Figure 4C).

Similar to that observed with 3-MA, incubation of the patients' cells cultured at 40 °C with the late autophagy inhibitor chloroquine (CQ) also resulted in increased levels of processed thiolase and ABCD1 (Figure 5A), as well as a correction of the number of cells with catalase- and ABCD3-containing peroxisomes to the level observed in cells cultured at 37 °C without inhibitor (Figure 5B and Supplemental Figure 2).

In addition to the established global autophagy inhibitors 3-MA and CQ, we also studied the effect of depleting NBR1 levels in the patients' cells. Previous work identified NBR1 as the main autophagy receptor involved in pexophagy.[29] To this end, we stably expressed an shRNA against *NBR1* in the fibroblasts from the patients, a PEX14-null patient and 2 control subjects, resulting in ~70%-85% reduction of *NBR1* mRNA (Supplemental Figure 3). Similar to that observed for 3-MA and CQ treatment, the NBR1 depletion resulted in increased levels of processed thiolase and ABCD1 both at 37 °C and 40 °C (Figure 5C), and, in cells cultured at 40 °C, correction of the number of cells with catalase- and ABCD3-containing peroxisomes to the level observed in cells cultured at 37 °C (Figure 5D and Supplemental Figure 4).

Finally, using the same incubation conditions as for the Red-Green lysosome pexophagy assay, we studied the effect of inhibiting lysosomal proteases on processed thiolase and ABCD1 in fibroblasts from the patients, a PEX14-null

Figure 3 Patient cells lose peroxisomes at 40 °C. A. Immunofluorescence microscopy analysis to determine the subcellular location of the peroxisomal matrix protein catalase (green signal) and the peroxisomal membrane protein ABCD3 (red signal) in primary fibroblasts of the 2 heterozygous PEX14 patients (patient 1 and patient 2), 1 previously reported PEX14-null patient (PEX14(2)), and a control individual. Cells were cultured at 37 °C or 40 °C. Shown are representative images (scale bar, 10 μm). B-D. Immunoblot analysis of homogenates prepared from primary fibroblasts of the 2 heterozygous PEX14 patients, 2 previously reported PEX14-null patients (PEX14(1) and PEX14(2)), and 2 control individuals cultured at 37 °C or 40 °C. Immunoblots were stained with antibodies against (B) PEX14, (C) the peroxisomal matrix proteins thiolase and ACOXI, and (D) the peroxisomal membrane proteins ABCD1 and ABCD5. As loading controls, the same blots were re-probed with antibodies against tubulin or β-actin as indicated. Performed in triplicate; shown are representative immunoblots. (E) Results of Red-Green pexophagy assay performed in fibroblasts of the 2 heterozygous PEX14 patients (patient 1 (P1) and patient 2 (P2)) and 2 control individuals (C1 and C2), transfected with mCherry-GFP-SKL, incubated for 4 days with lysosomal inhibitors (2 μM E-64, 500 μM Leupeptin) and examined by fluorescent microscopy. Cells were cultured at 37 °C. In total, images of 100 cells per fibroblast cell line were analyzed obtained from 3 independent experiments (25-40 per experiment). Data presented as percentage of cells with increased pexophagy, defined as cells >20% of orange/red pixels (see Supplemental Figure 1 for example images).

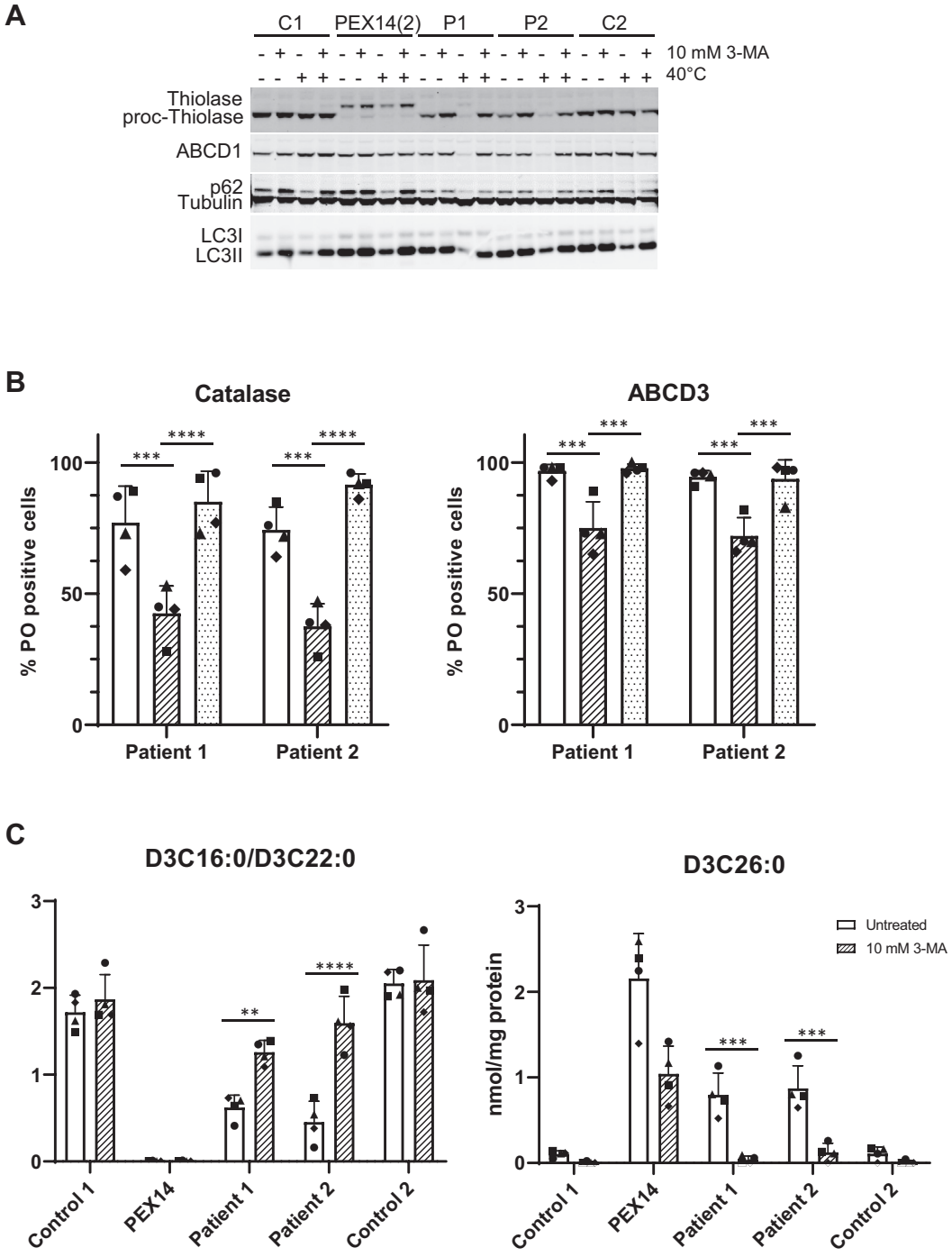

Figure 4 Rescue of functional peroxisomes by early autophagy inhibitor 3-MA. A. Immunoblot analysis of homogenates prepared from primary fibroblasts of the 2 heterozygous PEX14 patients (Patient 1 (P1) and Patient 2 (P2)), 1 previously reported PEX14-null patient (PEX14(2)), and 2 control individuals (C1 and C2) cultured at 37 °C and 40 °C. Cells were incubated with 10 mM 3-methyladenine (3-MA) for 7 days. Immunoblots were stained with antibodies against the peroxisomal matrix protein thiolase, the peroxisomal membrane protein ABCD1, the autophagy adaptor protein SQSTM1/P62 (P62), MAPILC3B (LC3I and LC3II), and, as loading control, tubulin. Performed in triplicate; shown are representative immunoblots. B. Percentage of patients' cells with catalase- or ABCD3-stained peroxisomes when cultured at 37 °C (white bars), or 7 days at 40 °C in the absence (dashed bars) or presence (stippled bars) of 10 mM 3-MA. Cells were examined with immunofluorescence microscopy to determine the subcellular location of the peroxisomal matrix protein catalase and the peroxisomal membrane protein ABCD3 (for examples see Supplemental Figure 2). Performed in quadruplicate; for each condition 100 cells were examined (total of 400 cells) (Two-way Anova with Tukey's multiple comparisons test, $P = .0002$, indicated by ***, $P < .0001$, indicated by ****). C. Peroxisomal fatty acid β-oxidation capacity, expressed as $D_3C16:0/D_3C22:0$ ratio, and $D_3C26:0$ levels measured in primary human fibroblasts of the 2 heterozygous PEX14 patients, 1 previously reported PEX14-null patient (PEX14(2)), and 2 control individuals. Cells were incubated for 72 hours with 30 μM D3-C22:0 at 40 °C in the absence (white bars) or the presence (dashed bars) of 10 mM 3-MA followed by fatty acid analysis (Two-way Anova with Sidak's multiple comparisons test, $P = .0021$, indicated by **, $P = .0002$, indicated by ***, $P < .0001$, indicated by ****).

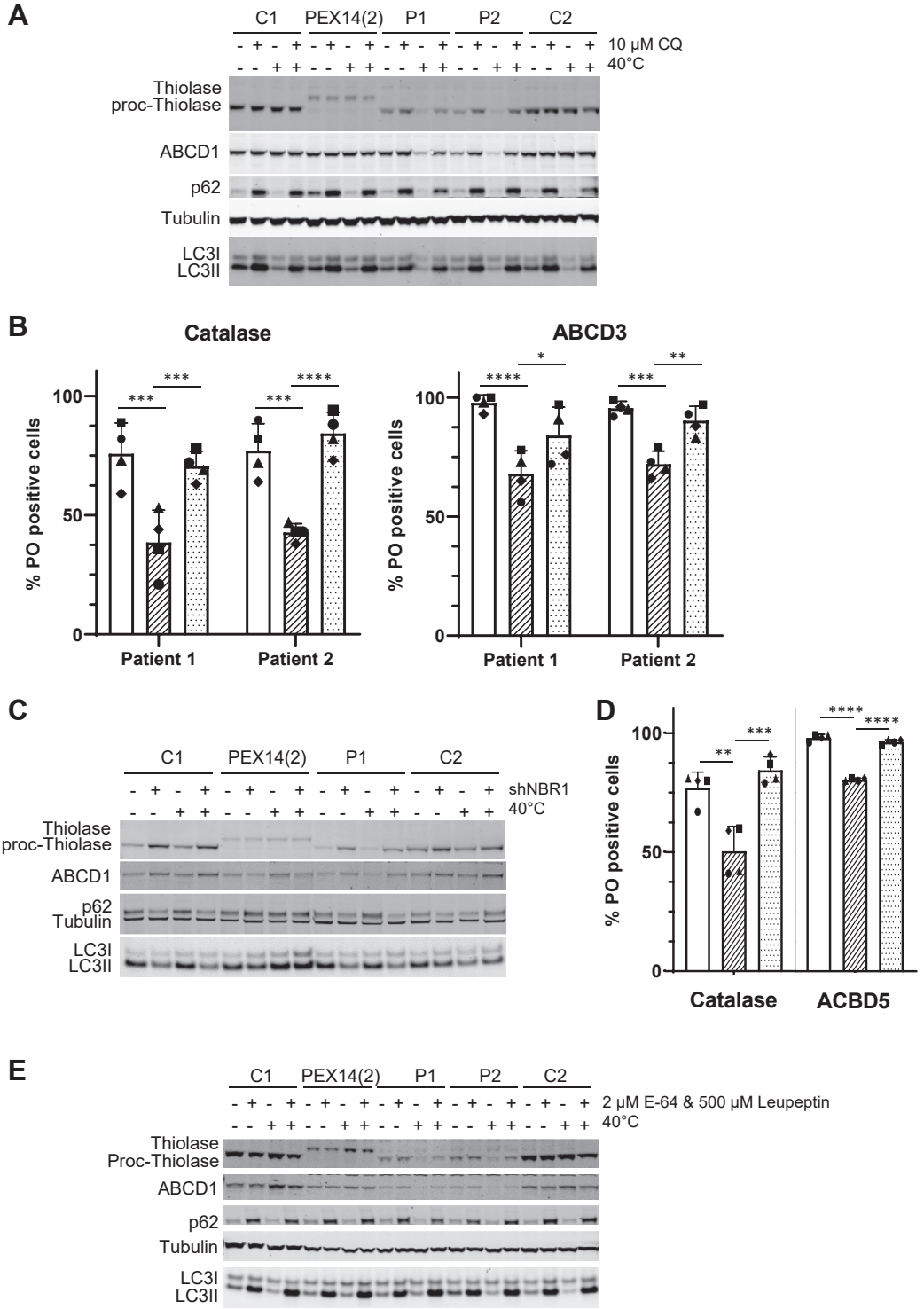

Figure 5 **Rescue of functional peroxisomes by late autophagy inhibitor chloroquine and genetic knockdown of *NBR1*.** A. Immunoblot analysis of homogenates prepared from primary fibroblasts of the 2 heterozygous PEX14 patients (patient 1 (P1) and patient 2 (P2)), 1 previously reported PEX14-null patient (PEX14(2)), and 2 control individuals (C1 and C2) cultured at 37 °C and 40 °C. Cells were incubated with 10 μM chloroquine (CQ) for 7 days. Immunoblots were stained with antibodies against the peroxisomal matrix protein thiolase, the peroxisomal membrane protein ABCD1, the autophagy adaptor protein SQSTM1/P62 (P62), MAPILC3B (LC3I and LC3II), and, as loading control, tubulin. Performed in triplicate; shown are representative immunoblots. B. Percentage of patients' cells with catalase- or ABCD3-stained peroxisomes when cultured at 37 °C (white bars), or 7 days at 40 °C in the absence (dashed bars) or presence (stippled bars) of 10 mM CQ. Cells were examined with immunofluorescence microscopy to determine the subcellular location of the peroxisomal matrix protein catalase and the peroxisomal membrane protein ABCD3 (for examples, see Supplemental Figure 2). Performed in quadruplicate; for each condition 100 cells were examined (total of 400 cells) (Two-way anova with Tukey's multiple comparisons test, $P = .0332$, indicated by *,

patient and 2 control subjects. Again and similar to that observed in the experiments with 3-MA, CQ, and depleted NBR1, we observed increased levels of processed thiolase and ABCD1 both at 37 °C and 40 °C, similar to the levels observed in cells cultured at 37 °C (Figure 5E).

Taken together, the finding that inhibition at different stages of autophagy all rescues the peroxisomal defect in the patients' cells indicate that the defective peroxisomal functions and global decrease in peroxisomal proteins in the patients' cells are predominantly a consequence of increased pexophagy.

Discussion

In this manuscript, we report 2 patients with an autosomal dominant ZSD due to 2 different single heterozygous splicing variants in *PEX14*. The dominant-negative pathogenic consequence of the variants was suggested by their de novo occurrence and the observation that they did not result in nonsense-mediated mRNA decay but produce stable C-terminally truncated PEX14 proteins. Subsequent expression studies confirmed that the truncated PEX14 proteins cannot functionally rescue the peroxisomal matrix protein import defect in PEX14-deficient cells and, when overexpressed in wild-type cells, result in a peroxisomal mosaic phenotype similar as in the patients' cells.

Mammalian PEX14 and PEX13 form the PEX5-docking complex of the so-called peroxisomal docking/translocation module, a transient hydrophilic pore that allows the translocation of newly synthesized peroxisomal matrix proteins into the peroxisomal lumen. The PEX5-docking complex is not involved in the import of peroxisomal membrane proteins, which also follows from the observation that PEX14-null and PEX13-null cells still have peroxisomal membrane vesicles that contain peroxisomal membrane proteins but lack imported matrix proteins. PEX14 and PEX13 have been found to interact with each other and with PEX5.[30] Previous studies with CHO cells showed that PEX5 accumulated at the membrane of peroxisomal ghosts in *PEX13* but remained cytosolic in *PEX14* mutant CHO cells,[28] based on which PEX14 was postulated to function as the actual docking protein for PEX5. However, opposite to these findings, we found that PEX5 accumulated at the peroxisomal membrane in PEX14-null but remained cytosolic in PEX13-null fibroblasts. We have no explanation for this striking difference between CHO and human cells. Although our findings do not exclude PEX14 as the actual PEX5 docking protein, they indicate that, at least in human primary fibroblasts, PEX13 is required for PEX5 docking and that, in the absence of PEX14, PEX5 can still dock on PEX13. In the cells of the heterozygous PEX14 patients, however, PEX5 remains cytosolic, indicating that the cycling of the receptor is not affected. This corroborates our finding that the peroxisomal matrix protein import machinery is still functional in the patients' cells, as underscored by the correct post-import processing of peroxisomal ACOX1 and thiolase. Yet, although truncated PEX14 can still interact with its known partners PEX5, PEX19, PEX13, and PEX14,[26] it cannot functionally rescue PEX14-null cells. This implies that the functional peroxisomal matrix protein import observed in the patients' cells is maintained by wild-type PEX14 expressed by the *trans* allele.

Our combined results strongly indicate that the truncated PEX14 proteins cause increased pexophagy resulting in increased degradation of protein import-proficient and metabolic functional peroxisomes in the heterozygous PEX14 patients' cells, but did not reveal an effect on peroxisomal protein import. In contrast to the other peroxisomal proteins, however, catalase was found both in peroxisomes and the cytosol of the cells. This is most probably not caused by a protein import defect but can be explained by the previously demonstrated reduced peroxisomal import rate of monomeric catalase.[31-33] This is due to the C-terminal–KANL peptide sequence of catalase that deviates from the consensus PTS1 consensus sequence and which was shown to have a lower affinity with PEX5.[31,32] The reduced import rate promotes the assembly into active

$P = .0021$, indicated by **, $P = .0002$, indicated by ***, $P < .0001$, indicated by ****). C. Immunoblot analysis of homogenates prepared from primary fibroblasts of 1 of the heterozygous PEX14 patients (patient 1 (P1)), 1 previously reported PEX14-null patient (PEX14(2)), and 2 control individuals (C1 and C2) cultured at 37 °C or 7 days at 40 °C. All cells stably express *NBR1*-specific short hairpin RNAs resulting in a 70%-85% decrease in the expression of the peroxisomal autophagy receptor NBR1 (Supplemental Figure 3). Immunoblots were stained with antibodies against the peroxisomal matrix protein thiolase, the peroxisomal membrane protein ABCD1, the autophagy adaptor protein SQSTM1/P62 (P62), MAPILC3B (LC3I and LC3II), and, as loading control, tubulin. Performed in triplicate; shown are representative immunoblots. D. Percentage of patient 1 cells with catalase- or ACBD5-stained peroxisomes when cultured at 37 °C (white bars) or 7 days at 40 °C (dashed bars) and of patient 1 cells stably expressing NBR1-specific shRNA cultured 7 days at 40 °C (stippled bars). Cells were examined with immunofluorescence microscopy to determine the subcellular location of the peroxisomal matrix protein catalase and the peroxisomal membrane protein ACBD5 (for examples see Supplemental Figure 4). Performed in quadruplicate; for each condition 100 cells were examined (total of 400 cells). (Two-way anova with Tukey's multiple comparisons test, $P = .0021$, indicated by **, $P = .0002$, indicated by ***, $P < .0001$, indicated by ****). E. Immunoblot analysis of homogenates prepared from primary fibroblasts of the 2 heterozygous PEX14 patients (patient 1 (P1) and patient 2 (P2)), 1 previously reported PEX14-null patient (PEX14(2)), and 2 control individuals (C1 and C2) pre-cultured at 37 °C or 7 days at 40 °C, and then incubated for 4 days with lysosomal inhibitors (2 μM E-64, 500 μM Leupeptin) as indicated. Immunoblots were stained with antibodies against the peroxisomal matrix protein thiolase, the peroxisomal membrane protein ABCD1, the autophagy adaptor protein SQSTM1/P62 (P62), MAPILC3B (LC3I and LC3II), and, as loading control, tubulin. Performed in triplicate; shown are representative immunoblots.

tetrameric proteins in the cytosol, which subsequently are imported into peroxisomes.[32,33] The increased pexophagy in the heterozygous PEX14 patients' cells lowers the number of protein import-proficient peroxisomes as a consequence of which the amount of catalase in the cytosol becomes increased. This is supported by the observation that the inhibition of autophagy/pexophagy in the patients' cells fully restored the peroxisomal import of catalase, despite the presence of truncated PEX14 (Figures 4 and 5).

Increased pexophagy has been reported previously in ZSD cells with pathogenic variants in the *PEX1*, *PEX6*, or *PEX26* genes. In contrast to what we observed in the cells of the heterozygous PEX14 patients, however, this always coincides with defective peroxisome biogenesis, including, in particular, defective peroxisomal matrix protein import and, as a consequence, affected peroxisomal metabolic functions. This strongly suggests that, in these cells, the pexophagy is triggered by non-functional peroxisomes.[3,18,23,34] Although it had been claimed, based primarily on morphological data, that inhibition of pexophagy with autophagy inhibitors leads to improved peroxisomal functioning in ZSD cells harboring the common PEX1-p.(Gly843Asp) variant,[23] this could not be confirmed by detailed analyses of peroxisomal matrix protein import and actual peroxisomal metabolic functions in such cells treated with the same autophagy inhibitors.[18] Here, however, we found that inhibition at different stages of autophagy/pexophagy in cells of the heterozygous PEX14 patients all prevented the increased degradation of protein import-proficient and metabolic functional peroxisomes and thus resulted in improved peroxisomal functions in the cells. These findings suggest that, for these 2 patients, treatment with autophagy inhibitors, including CQ, may be a therapeutic option.

How and why the truncated PEX14 proteins increase pexophagy in the patients' cells remains unclear. PEX14 has been reported previously to play a dual role in both peroxisomal matrix protein import and pexophagy.[35,36] Studies in CHO cells indicated that during nutrient-deprivation, PEX14 interacts with LC3II via its N-terminal transmembrane domain, which then targets the peroxisomes to autophagosomes resulting in their degradation. During nutrient-rich conditions, this interaction with LC3II was prevented by PEX5. Based on these findings, PEX14 was postulated to coordinate the fate of peroxisomes, ie, matrix protein import versus pexophagy, in response to environmental conditions.[35,36] This PEX14-mediated pexophagy is independent of ubiquitin in contrast to the other currently known modes of pexophagy, which are all ubiquitin dependent and involve the participation of ubiquitin-binding autophagic receptors, such as NBR1 and P62.[3,29,37] Our observation that truncated PEX14 can still bind PEX5 and that the depletion of NBR1 rescues the phenotype in the patients' cells makes it unlikely that this previously reported PEX14-mediated mechanism is responsible for the increased pexophagy in the patients' cells.

Most peroxisomal disorders we know to date are autosomal recessively inherited and thus caused by bi-allelic pathogenic variants in the same gene.[6] Exceptions are X-linked recessive adrenoleukodystrophy, the most common peroxisomal disorder,[38] and autosomal dominant DNM1 deficiency, which affects fission of both peroxisomes and mitochondria.[39] More recently, we reported a series of patients with an apparent dominant ZSD presentation, which appeared to be caused by allelic expression imbalance of the *PEX6* gene. All patients were heterozygous for a pathogenic PEX6-p.(Arg860Trp) variant, which was expressed in trans with a lower expressed *PEX6* allele. This results in overrepresentation of PEX6-p.(Arg860Trp), which thus exerts a dominant-negative effect on the function of the PEX1-PEX6 complex, affecting peroxisomal matrix protein import.[40]

Our finding of a true autosomal dominant form of ZSD in 2 independent patients expands the genetic repertoire underlying ZSD and, more general, underscores that single heterozygous variants should not be ignored as possible genetic cause of diseases with an established autosomal recessive mode of inheritance.

Data Availability

The data supporting the findings of this study are available within the article and/or its Supplemental Material or can be made available upon request.

Acknowledgments

We thank Petra Mooijer and Conny Dekker for technical assistance and acknowledge Gaby Dodt, Marc Fransen, and Denis Crane for provision of antibodies.

Funding

This work was supported in part by E-Rare-3 Joint Translational Call PERescue (2015) supported by The Netherlands Organization for Health Research and Development (ZonMW; H.R.W. and J.K.).

J.Z. and S.K. were supported by grant NV19-07-00136 from the Ministry of Health of the Czech Republic and acknowledge The National Center for Medical Genomics (LM2018132) for instrumental and methodologic support with the exome sequencing analyses. P.J. was supported by the institutional grant RVO VFN64165 from the Ministry of Health of the Czech Republic.

Author Information

Conceptualization: H.R.W., J.K., S.F.; Formal Analysis: H.R.W., J.K., S.F.; Investigation: J.K., M.S.E., J.Z., L.N., S.K., P.D., D.C., S.F.; Methodology: H.R.W., J.K.; Project administration: H.R.W.; Resources: P.J., J.Z., S.K., P.D.,

D.C.; Supervision: H.R.W.; Visualization: H.R.W., J.K.; Writing – original draft: H.R.W., J.K.; Writing – review & editing: H.R.W., J.K., M.S.E., R.J.A.W., S.F.

Ethics Declaration

The study on patient 1 was approved by the Ethics committee of the General University Hospital in Prague and was conducted in agreement with the Declaration of Helsinki and institutional guidelines. Written informed consent for molecular analyses was obtained from the patient and his mother.

The study on patient 2 was conducted in agreement with the Declaration of Helsinki and institutional guidelines. A specific written informed consent for molecular analyses was obtained from the patient.

The Medical Ethics Review Committee of the Amsterdam UMC, where most of the laboratory diagnostics and all functional studies have been performed, has indicated that functional follow-up studies do not require their official approval, because these studies are not considered 'research with or involving human subjects' and thus the 'Medical Research Involving Human Subjects Act' (WMO) does not apply.

Conflict of Interest

The authors declare no conflicts of interest.

Additional Information

The online version of this article (https://doi.org/10.1016/j.gim.2023.100944) contains supplemental material, which is available to authorized users.

Affiliations

[1]Amsterdam UMC - AMC, Department of Laboratory Medicine, Laboratory Genetic Metabolic Diseases, Amsterdam, The Netherlands; [2]Amsterdam Gastroenterology Endocrinology Metabolism, Amsterdam, The Netherlands; [3]Amsterdam Reproduction & Development, Amsterdam, The Netherlands; [4]United for Metabolic Diseases, The Netherlands; [5]Department of Pediatrics and Inherited Metabolic Disorders, First Faculty of Medicine, Charles University and General Faculty Hospital, Prague 2, Czech Republic; [6]Centre Hospitalier Universitaire de Lyon, CHU Lyon·U 301, Hopital Neurologique, Bron, France; [7]Service Biochimie et Biologie Moléculaire Grand Est, UM Pathologies Métaboliques, Erythrocytaires et Dépistage Périnatal, Centre de Biologie et de Pathologie Est, Groupement Hospitalier Est – Hospices Civils de Lyon, Bron Cedex, France

References

1. Wanders RJ, Waterham HR. Biochemistry of mammalian peroxisomes revisited. *Annu Rev Biochem*. 2006;75:295-332. http://doi.org/10.1146/annurev.biochem.74.082803.133329
2. Huybrechts SJ, Van Veldhoven PP, Brees C, Mannaerts GP, Los GV, Fransen M. Peroxisome dynamics in cultured mammalian cells. *Traffic*. 2009;10(11):1722-1733. http://doi.org/10.1111/j.1600-0854.2009.00970.x
3. Germain K, Kim PK. Pexophagy: a model for selective autophagy. *Int J Mol Sci*. 2020;21(2). http://doi.org/10.3390/ijms21020578
4. Schrader M, Costello JL, Godinho LF, Azadi AS, Islinger M. Proliferation and fission of peroxisomes – an update. *Biochim Biophys Acta*. 2016;1863(5):971-983. http://doi.org/10.1016/j.bbamcr.2015.09.024
5. Farré JC, Mahalingam SS, Proietto M, Subramani S. Peroxisome biogenesis, membrane contact sites, and quality control. *EMBO Rep*. 2019;20(1). http://doi.org/10.15252/embr.201846864
6. Waterham HR, Ferdinandusse S, Wanders RJ. Human disorders of peroxisome metabolism and biogenesis. *Biochim Biophys Acta*. 2016;1863(5):922-933. http://doi.org/10.1016/j.bbamcr.2015.11.015
7. Klouwer FC, Berendse K, Ferdinandusse S, Wanders RJ, Engelen M, Poll-The BT. Zellweger spectrum disorders: clinical overview and management approach. *Orphanet J Rare Dis*. 2015;10:151. http://doi.org/10.1186/s13023-015-0368-9
8. Braverman NE, Raymond GV, Rizzo WB, et al. Peroxisome biogenesis disorders in the Zellweger spectrum: an overview of current diagnosis, clinical manifestations, and treatment guidelines. *Mol Genet Metab*. 2016;117(3):313-321. http://doi.org/10.1016/j.ymgme.2015.12.009
9. Ferdinandusse S, Ebberink MS, Vaz FM, Waterham HR, Wanders RJ. The important role of biochemical and functional studies in the diagnostics of peroxisomal disorders. *J Inherit Metab Dis*. 2016;39(4):531-543. http://doi.org/10.1007/s10545-016-9922-4
10. Waterham HR, Ebberink MS. Genetics and molecular basis of human peroxisome biogenesis disorders. *Biochim Biophys Acta*. 2012;1822(9):1430-1441. http://doi.org/10.1016/j.bbadis.2012.04.006
11. Shimozawa N, Tsukamoto T, Nagase T, et al. Identification of a new complementation group of the peroxisome biogenesis disorders and PEX14 as the mutated gene. *Hum Mutat*. 2004;23(6):552-558. http://doi.org/10.1002/humu.20032
12. Huybrechts SJ, Van Veldhoven PP, Hoffman I, et al. Identification of a novel PEX14 mutation in Zellweger syndrome. *J Med Genet*. 2008;45(6):376-383. http://doi.org/10.1136/jmg.2007.056697
13. Ebberink MS, Mooijer PA, Gootjes J, Koster J, Wanders RJ, Waterham HR. Genetic classification and mutational spectrum of more than 600 patients with a Zellweger syndrome spectrum disorder. *Hum Mutat*. 2011;32(1):59-69. http://doi.org/10.1002/humu.21388
14. Dacremont G, Cocquyt G, Vincent G. Measurement of very long-chain fatty acids, phytanic and pristanic acid in plasma and cultured fibroblasts by gas chromatography. *J Inherit Metab Dis*. 1995;18(suppl 1):76-83. http://doi.org/10.1007/BF00711430
15. Klouwer FCC, Ferdinandusse S, van Lenthe H, et al. Evaluation of C26:0-lysophosphatidylcholine and C26:0-carnitine as diagnostic markers for Zellweger spectrum disorders. *J Inherit Metab Dis*. 2017;40(6):875-881. http://doi.org/10.1007/s10545-017-0064-0
16. Ofman R, Wanders RJ. Purification of peroxisomal acyl-CoA: dihydroxyacetonephosphate acyltransferase from human placenta. *Biochim Biophys Acta*. 1994;1206(1):27-34. http://doi.org/10.1016/0167-4838(94)90068-x
17. van de Beek MC, Dijkstra IM, Kemp S. Method for measurement of peroxisomal very long-chain fatty acid beta-oxidation and de novo C26:0 synthesis activity in living cells using stable-isotope labeled docosanoic acid. *Methods Mol Biol*. 2017;1595:45-54. http://doi.org/10.1007/978-1-4939-6937-1_5

18. Klouwer FCC, Falkenberg KD, Ofman R, et al. Autophagy inhibitors do not restore peroxisomal functions in cells with the most common peroxisome biogenesis defect. *Front Cell Dev Biol*. 2021;9:661298. http://doi.org/10.3389/fcell.2021.661298
19. van Grunsven EG, van Berkel E, Mooijer PA, et al. Peroxisomal bifunctional protein deficiency revisited: resolution of its true enzymatic and molecular basis. *Am J Hum Genet*. 1999;64(1):99-107. http://doi.org/10.1086/302180
20. Wiemer EA, Ofman R, Middelkoop E, de Boer M, Wanders RJ, Tager JM. Production and characterisation of monoclonal antibodies against native and disassembled human catalase. *J Immunol Methods*. 1992;151(1-2):165-175. http://doi.org/10.1016/0022-1759(92)90115-a
21. Hartmannová H, Piherová L, Tauchmannová K, et al. Acadian variant of Fanconi syndrome is caused by mitochondrial respiratory chain complex I deficiency due to a non-coding mutation in complex I assembly factor NDUFAF6. *Hum Mol Genet*. 2016;25(18):4062-4079. http://doi.org/10.1093/hmg/ddw245
22. Ferdinandusse S, Falkenberg KD, Koster J, et al. ACBD5 deficiency causes a defect in peroxisomal very long-chain fatty acid metabolism. *J Med Genet*. 2017;54(5):330-337. http://doi.org/10.1136/jmedgenet-2016-104132
23. Law KB, Bronte-Tinkew D, Di Pietro E, et al. The peroxisomal AAA ATPase complex prevents pexophagy and development of peroxisome biogenesis disorders. *Autophagy*. 2017;13(5):868-884. http://doi.org/10.1080/15548627.2017.1291470
24. Imamura A, Tsukamoto T, Shimozawa N, et al. Temperature-sensitive phenotypes of peroxisome-assembly processes represent the milder forms of human peroxisome-biogenesis disorders. *Am J Hum Genet*. 1998;62(6):1539-1543. http://doi.org/10.1086/301881
25. Imamura A, Tamura S, Shimozawa N, et al. Temperature-sensitive mutation in PEX1 moderates the phenotypes of peroxisome deficiency disorders. *Hum Mol Genet*. 1998;7(13):2089-2094. http://doi.org/10.1093/hmg/7.13.2089
26. Azevedo JE, Pex SW. 14p, more than just a docking protein. *Biochim Biophys Acta*. 2006;1763(12):1574-1584.
27. Dodt G, Gould SJ. Multiple PEX genes are required for proper subcellular distribution and stability of Pex5p, the PTS1 receptor: evidence that PTS1 protein import is mediated by a cycling receptor. *J Cell Biol*. 1996;135(6 Pt 2):1763-1774. http://doi.org/10.1083/jcb.135.6.1763
28. Otera H, Harano T, Honsho M, et al. The mammalian peroxin Pex5pL, the longer isoform of the mobile peroxisome targeting signal (PTS) type 1 transporter, translocates the Pex7p.PTS2 protein complex into peroxisomes via its initial docking site, Pex14p. *J Biol Chem*. 2000;275(28):21703-21714. http://doi.org/10.1074/jbc.M000720200
29. Deosaran E, Larsen KB, Hua R, et al. NBR1 acts as an autophagy receptor for peroxisomes. *J Cell Sci*. 2013;126(4):939-952. http://doi.org/10.1242/jcs.114819
30. Barros-Barbosa A, Ferreira MJ, Rodrigues TA, et al. Membrane topologies of PEX13 and PEX14 provide new insights on the mechanism of protein import into peroxisomes. *FEBS Journal*. 2019;286(1):205-222. http://doi.org/10.1111/febs.14697
31. Fujiwara C, Imamura A, Hashiguchi N, et al. Catalase-less peroxisomes. Implication in the milder forms of peroxisome biogenesis disorder. *J Biol Chem*. 2000;275(47):37271-37277. http://doi.org/10.1074/jbc.M006347200
32. Koepke JI, Nakrieko KA, Wood CS, et al. Restoration of peroxisomal catalase import in a model of human cellular aging. *Traffic*. 2007;8(11):1590-1600. http://doi.org/10.1111/j.1600-0854.2007.00633.x
33. Williams C, Bener Aksam E, Gunkel K, Veenhuis M, van der Klei IJ. The relevance of the non-canonical PTS1 of peroxisomal catalase. *Biochim Biophys Acta*. 2012;1823(7):1133-1141. http://doi.org/10.1016/j.bbamcr.2012.04.006
34. Heikoop JC, van den Berg M, Strijland A, et al. Turnover of peroxisomal vesicles by autophagic proteolysis in cultured fibroblasts from Zellweger patients. *Eur J Cell Biol*. 1992;57(2):165-171.
35. Hara-Kuge S, Fujiki Y. The peroxin Pex14p is involved in LC3-dependent degradation of mammalian peroxisomes. *Exp Cell Res*. 2008;314(19):3531-3541. http://doi.org/10.1016/j.yexcr.2008.09.015
36. Jiang L, Hara-Kuge S, Yamashita S, Fujiki Y, Pex P. Peroxin Pex14p is the key component for coordinated autophagic degradation of mammalian peroxisomes by direct binding to LC3-II. *Genes Cells*. 2015;20(1):36-49. http://doi.org/10.1111/gtc.12198
37. Lamark T, Kirkin V, Dikic I, Johansen T. NBR1 and p62 as cargo receptors for selective autophagy of ubiquitinated targets. *Cell Cycle*. 2009;8(13):1986-1990. http://doi.org/10.4161/cc.8.13.8892
38. Mallack EJ, Gao K, Engelen M, Kemp S. Structure and function of the ABCD1 variant database: 20 years, 940 pathogenic variants, and 3400 cases of adrenoleukodystrophy. *Cells*. 2022;11(2). http://doi.org/10.3390/cells11020283
39. Waterham HR, Koster J, van Roermund CW, Mooyer PA, Wanders RJ, Leonard JV. A lethal defect of mitochondrial and peroxisomal fission. *N Engl J Med*. 2007;356(17):1736-1741. http://doi.org/10.1056/NEJMoa064436
40. Falkenberg KD, Braverman NE, Moser AB, et al. Allelic expression imbalance promoting a mutant PEX6 allele causes Zellweger spectrum disorder. *Am J Hum Genet*. 2017;101(6):965-976. http://doi.org/10.1016/j.ajhg.2017.11.007